

## Ab Initio MO Study of the Thermal Decomposition of Fluorinated Disilanes,

 $\text{Si}_2\text{H}_{6-n}\text{F}_n$  ( $n = 0, 1, 2$ )Edgar W. Ignacio<sup>†</sup> and H. Bernhard Schlegel\*

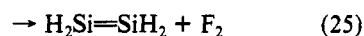
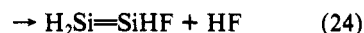
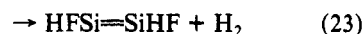
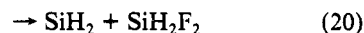
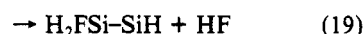
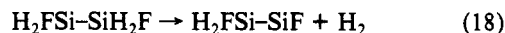
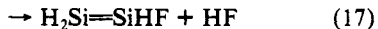
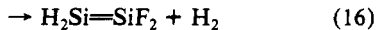
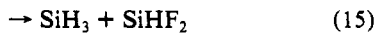
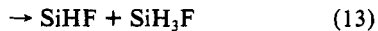
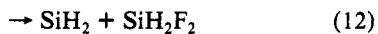
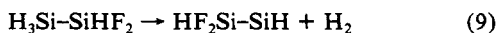
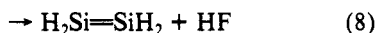
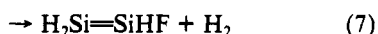
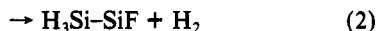
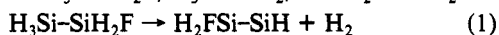
Department of Chemistry, Wayne State University, Detroit, Michigan 48202 (Received: July 16, 1991)

The reactants, transition structures, and products for the various channels for the thermal decomposition of  $\text{Si}_2\text{H}_{6-n}\text{F}_n$  were optimized at the HF/3-21G and HF/6-31G\* levels. The electron correlation contributions were calculated at the MP4/6-31G\* level with the zero-point energies at the HF/3-21G level. Isodesmic reactions have been used to estimate the heats of formation of  $\text{SiH}_3\text{SiH}_2\text{F}$ ,  $\text{SiH}_2\text{FSiH}_2\text{F}$ ,  $\text{SiH}_3\text{SiHF}_2$ ,  $\text{SiH}_2\text{FSiH}$ ,  $\text{SiHF}_2\text{SiH}$ ,  $\text{SiH}_3\text{SiF}$ , and  $\text{SiH}_2\text{FSiF}$ . In the decomposition of disilane, the  $\text{SiH}_2 + \text{SiH}_4$  and  $\text{SiH}_3\text{SiH} + \text{H}_2$  paths are favored over other modes of decomposition. For monofluorodisilane, the  $\text{SiH}_3\text{F} + \text{SiH}_2$ ,  $\text{SiH}_2\text{FSiH} + \text{H}_2$ , and  $\text{SiH}_3\text{SiF} + \text{H}_2$  channels are nearly equal in energy and are preferred over  $\text{SiH}_4 + \text{SiHF}$ . In the decomposition of the 1,1-difluorodisilane,  $\text{SiH}_3\text{SiHF}_2$ , the barriers for decomposition into  $\text{SiH}_2\text{F}_2 + \text{SiH}_2$ ,  $\text{SiHF}_2\text{SiH} + \text{H}_2$ , and  $\text{SiH}_3\text{F} + \text{SiHF}$  are very close in energy, while the  $\text{SiH}_4 + \text{SiF}_2$  channel is considerably higher. In the decomposition of the 1,2-difluorodisilane,  $\text{SiH}_2\text{FSiH}_2\text{F}$ , the barriers for decomposition into  $\text{SiH}_2\text{F}_2 + \text{SiH}_2$ ,  $\text{SiH}_2\text{FSiF} + \text{H}_2$ , and  $\text{SiH}_3\text{F} + \text{SiHF}$  are similar in energy. For all the fluorodisilanes considered, the barriers for the elimination of HF and the homolytic cleavage of the Si-Si bond are considerably higher than those of the elimination of  $\text{H}_2$  or the extrusion of a silylene.

## Introduction

Fluorinated silanes and disilanes, and reactive intermediates derived from these compounds, are important in chemical vapor deposition and etching of silicon surfaces (for some leading refs, see 1-4). The pathways for thermal decomposition of fluorinated monosilanes were discussed in a previous paper.<sup>5</sup> In addition to these processes, disilanes can undergo homolytic Si-Si bond rupture, SiXY extrusion, and 1,2-elimination of  $\text{H}_2$  and HF. A previous study on the thermal decomposition of disilane by Gordon et al.<sup>6</sup> found that 1,1-elimination of  $\text{H}_2$  from  $\text{Si}_2\text{H}_6$  has a much lower barrier than 1,2-elimination, even though  $\text{H}_2\text{Si}=\text{SiH}_2$  is more stable than  $\text{H}_3\text{SiSiH}$ . Silylene insertion into  $\text{SiH}_4$  has been shown to occur with no barrier<sup>7</sup> whereas the barrier for insertion into the SiF bond of  $\text{SiH}_3\text{F}$ <sup>8</sup> is comparable to that of insertion into HF.<sup>9</sup> The addition of HF to silanol and fluorodisilane was studied recently to model etching of silicon surfaces.<sup>10</sup> Accurate theoretical estimates of the heats of formation are available for fluorine-substituted monosilanes<sup>11,12</sup> and for  $\text{Si}_2\text{H}_n$ .<sup>12,13,14</sup> Unimolecular dissociation dynamics have been studied theoretically for disilane.<sup>15</sup>

In this paper, we explore a number of pathways for the thermal decomposition of  $\text{H}_3\text{SiSiH}_2\text{F}$ ,  $\text{H}_3\text{SiSiHF}_2$ , and  $\text{H}_2\text{FSiSiH}_2\text{F}$ :



Reactions 6, 15, and 22 are homolytic bond cleavage reactions and can be assumed to have little or no barrier in the reverse direction. The reverse of reactions 1, 2, 9, and 18 are insertion reactions into  $\text{H}_2$ , while the reverse of reactions 3, 10, and 19 are insertions into HF. Decomposition reactions yielding  $\text{F}_2$  are too high in energy<sup>5</sup> and hence are not considered here. The other categories are insertions of  $\text{SiH}_2$  into  $\text{SiH}_{4-n}\text{F}_n$  (reactions 4, 12, and 20), insertions of SiHF into  $\text{SiH}_{4-n}\text{F}_n$  (reactions 5, 13, and 21), and insertion of  $\text{SiF}_2$  in  $\text{SiH}_4$  (reaction 14). The 1,2-elimination of  $\text{H}_2$  from  $\text{Si}_2\text{H}_6$  was studied by Gordon et al.<sup>6</sup> and found to have a very high barrier; the 1,2-elimination of HF is expected to have a similarly high barrier. Hence 1,2-eliminations are not considered in this study.

(1) Patai, S.; Rappoport, Z., Eds. *The Chemistry of Organic Silicon Compounds*; Wiley: New York, 1989.

(2) Corey, E. R.; Gaspar, P. P., Eds. *Silicon Chemistry*; Ellis Horwood: Chichester, England, 1988.

(3) Jasinski, J. M.; Meyerson, B. S.; Scott, B. A. *Annu. Rev. Phys. Chem.* **1987**, *38*, 109.

(4) Pankove, J. I., Ed. *Semiconductors and Semimetals*; Academic: New York, 1984.

(5) Ignacio, E. W.; Schlegel, H. B. *J. Phys. Chem.*, this issue. Sosa, C.; Schlegel, H. B. *J. Am. Chem. Soc.* **1984**, *106*, 5847.

(6) Gordon, M. S.; Truong, T. N.; Bonderson, E. K. *J. Am. Chem. Soc.* **1986**, *108*, 1421.

(7) Gordon, M. S.; Gano, D. R. *J. Am. Chem. Soc.* **1984**, *106*, 5421.

(8) Schlegel, H. B.; Sosa, C. *J. Phys. Chem.* **1985**, *89*, 537.

(9) Raghavachari, K.; Chandrasekhar, J.; Gordon, M. S.; Dykema, K. *J. Am. Chem. Soc.* **1984**, *106*, 5853.

(10) Trucks, G. W.; Raghavachari, K.; Higashi, G. S.; Chabal, Y. *J. Phys. Rev. Lett.* **1990**, *65*, 504; *66*, 1648.

(11) Schlegel, H. B. *J. Phys. Chem.* **1984**, *88*, 6255. Ignacio, E. W.; Schlegel, H. B. *J. Chem. Phys.* **1990**, *92*, 5404.

(12) Ho, P.; Melius, C. F. *J. Phys. Chem.* **1990**, *94*, 5120.

(13) Curtiss, L. A.; Raghavachari, K.; Deutsch, P. W.; Pople, J. A. *J. Chem. Phys.* **1991**, *95*, 2433.

(14) Sax, A. F.; Kalcher, J. *J. Phys. Chem.* **1991**, *95*, 1768.

(15) Agrawal, P. M.; Thompson, D. L.; Raff, L. M. *J. Chem. Phys.* **1990**, *92*, 1069.

<sup>†</sup> Present address: Department of Chemistry, MSU-Iligan Institute of Technology, Iligan City, 9200 Philippines.

TABLE I: Total Energies<sup>a</sup>

molecule	3-21G		6-31G*			3-21G ZPE
	HF	HF	MP2	MP3	MP4	
Reactants						
$\text{H}_3\text{Si-SiH}_3$	-578.241 21	-581.305 09	-581.464 51	-581.497 30	-581.508 31	31.86
$\text{H}_3\text{Si-SiH}_2\text{F}$	-676.625 17	-680.225 84	-680.554 87	-680.579 93	-680.598 00	29.31
$\text{H}_3\text{Si-SiHF}_2$	-775.022 27	-779.158 11	-779.659 00	-779.676 49	-779.701 87	26.33
$\text{H}_2\text{FSi-SiH}_2\text{F}$ (anti)	-775.006 49	-779.146 25	-779.644 53	-779.661 88	-779.686 88	26.74
Products						
$\text{H}_3\text{Si-SiH}$	-577.038 70	-580.080 05	-580.225 71	-580.257 12	-580.268 15	19.78
$\text{H}_2\text{FSi-SiH}$	-675.420 87	-679.001 50	-679.317 02	-679.340 81	-679.358 83	17.26
$\text{HF}_2\text{Si-SiH}$	-773.812 68	-777.931 67	-778.418 46	-778.434 71	-778.459 92	14.32
$\text{H}_3\text{Si-SiF}$	-675.431 27	-679.007 10	-679.328 24	-679.351 02	-679.371 15	17.26
$\text{H}_2\text{FSi-SiF}$	-773.810 90	-777.927 32	-778.417 69	-778.432 87	-778.459 84	14.65
Transition States						
$\text{H}_3\text{Si-SiH-H}_2$	-578.127 12	-581.186 96	-581.365 64	-581.400 55	-581.412 62	29.24
$\text{H}_2\text{FSi-SiH-H}_2$	-676.513 53	-680.110 05	-680.458 75	-680.485 87	-680.504 98	26.79
$\text{HF}_2\text{Si-SiH-H}_2$	-774.908 67	-779.041 11	-779.562 33	-779.581 86	-779.608 38	23.60
$\text{H}_3\text{Si-SiF-H}_2$	-676.499 29	-680.095 73	-680.447 63	-680.474 62	-680.494 73	25.73
$\text{H}_2\text{FSi-SiF-H}_2$	-774.883 24	-779.018 21	-779.539 63	-779.559 01	-779.586 31	23.69
$\text{H}_3\text{Si-SiH-HF}$	-676.478 26	-680.410 59	-680.410 55	-680.433 26	-680.457 14	26.38
$\text{H}_2\text{FSi-SiH-HF}$	-774.861 69	-778.975 02	-779.500 73	-779.515 61	-779.546 59	23.92
$\text{H}_3\text{Si-SiF-HF}$	-774.865 56	-778.978 23	-779.507 26	-779.521 95	-779.554 04	23.05
$\text{H}_3\text{Si-H-SiH}_2$	-578.142 79	-581.211 67	-581.381 55	-581.415 53	-581.427 73	30.24
$\text{H}_2\text{FSi-H-SiH}_2$ (s)	-676.537 79	-680.143 22	-680.484 46	-680.510 19	-680.529 78	27.95
$\text{HF}_2\text{Si-H-SiH}_2$ (sg)	-774.932 42	-779.070 29	-779.583 03	-779.601 36	-779.628 28	25.08
$\text{H}_3\text{Si-H-SiHF}$	-676.520 02	-680.123 38	-680.463 86	-680.490 28	-680.510 22	27.77
$\text{H}_2\text{FSi-H-SiHF}$	-774.941 05	-779.055 31	-779.570 08	-779.585 31	-779.614 71	25.93
$\text{H}_3\text{Si-H-SiF}_2$	-774.903 08	-779.040 74	-779.551 42	-779.570 11	-779.607 69	24.66
$\text{H}_3\text{Si-F-SiH}_2$	-676.546 00	-680.127 81	-680.469 64	-680.492 87	-680.514 43	28.65
$\text{H}_2\text{FSi-F-SiH}_2$	-774.945 69	-779.063 43	-779.577 59	-779.593 23	-779.621 71	25.35
$\text{H}_3\text{Si-F-SiHF}$	-774.909 21	-779.049 05	-779.560 49	-779.578 58	-779.606 14	25.14

<sup>a</sup> In atomic units for total energies, kcal/mol for zero-point energies.

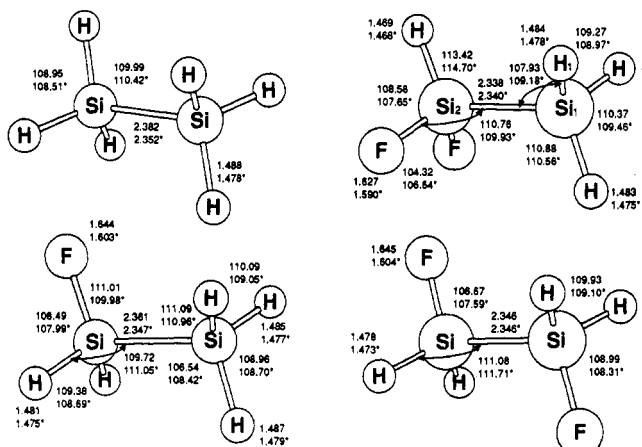


Figure 1. Optimized geometries of the fluorosilane reactants: no superscript, HF/3-21G; asterisk, HF/6-31G\*.

### Computational Method

Ab initio MO calculations were carried out with GAUSSIAN 88 and GAUSSIAN 90<sup>16</sup> with split valence (3-21G)<sup>17</sup> and polarization (6-31G\*)<sup>18</sup> basis sets. All geometries were fully optimized at the Hartree-Fock level with the 3-21G and 6-31G\* basis sets using analytical gradient methods.<sup>19</sup> Zero-point energies were obtained at the HF/3-21G level using analytical second derivatives. The

(16) Frisch, M. J.; Head-Gordon, M.; Trucks, G. W.; Foresman, J. B.; Schlegel, H. B.; Raghavachari, K.; Robb, M. A.; Binkley, J. S.; Gonzalez, C.; DeFrees, D. J.; Fox, D. J.; Whiteside, R. A.; Seeger, R.; Melius, C. F.; Baker, J.; Martin, L. R.; Kahn, L. R.; Stewart, J. J. P.; Topiol, S.; Pople, J. A. *Gaussian 90* Gaussian, Inc.: Pittsburgh, PA, 1990.

(17) Binkley, J. S.; Pople, J. A.; Hehre, W. J. *J. Am. Chem. Soc.* **1980**, *102*, 939. Gordon, M. S.; Binkley, J. S.; Pople, J. A.; Pietro, W. J.; Hehre, W. J. *J. Am. Chem. Soc.* **1982**, *104*, 2797.

(18) Hariharan, P. C.; Pople, J. A. *Theor. Chem. Acta* **1973**, *28*, 213. Franci, M. M.; Pietro, W. J.; Hehre, W. J.; Binkley, J. S.; Gordon, M. S.; DeFrees, D. J.; Pople, J. A. *J. Chem. Phys.* **1982**, *77*, 3654 and references cited.

(19) Schlegel, H. B. *J. Comput. Chem.* **1982**, *3*, 214.

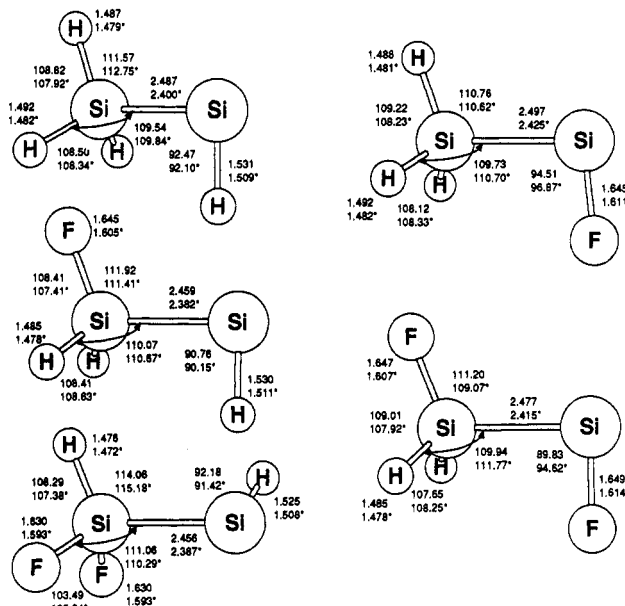


Figure 2. Optimized geometries of the fluorosilylsilylene products: no superscript, HF/3-21G; asterisk, HF/6-31G\*.

fourth-order Møller-Plesset perturbation theory<sup>20</sup> in the space of single, double, triple, and quadruple excitations (MP4SDTQ, frozen core) was used to estimate electron correlation energy with the 6-31G\* basis set.

### Results and Discussion

Table I presents the total energies of the disilane reactants, transition states, and products. Data for the monosilanes appearing in the products of reactions 1-25 have been published previously.<sup>5,11</sup>

(20) Pople, J. A.; Krishnan, R.; Schlegel, H. B.; Binkley, J. S. *Int. J. Quantum Chem., Quantum Chem. Symp.* **1979**, *13*, 225. For a review, see: Bartlett, R. J. *Annu. Rev. Phys. Chem.* **1981**, *32*, 359.

TABLE II: Barriers for Silylene Insertion Reactions<sup>a</sup>

reactions	3-21G	6-31G*				3-21G
	HF	HF	MP2	MP3	MP4	$\Delta ZPE$
$\text{HSiH} + \text{H}_2 \rightarrow \text{SiH}_4^b$		21.7	11.1	11.2	12.0	3.5
$\text{H}_3\text{Si-SiH} + \text{H}_2 \rightarrow \text{H}_3\text{Si-SiH}_3$	24.5	15.3	5.4	6.5	6.8	2.8
$\text{H}_2\text{FSi-SiH} + \text{H}_2 \rightarrow \text{H}_2\text{FSi-SiH}_2\text{F}$	21.9	14.4	4.4	5.5	5.8	2.9
$\text{HF}_2\text{Si-SiH} + \text{H}_2 \rightarrow \text{HF}_2\text{Si-SiH}_3$	19.6	13.2	2.6	3.6	3.8	2.6
$\text{HSiF} + \text{H}_2 \rightarrow \text{SiH}_3\text{F}^b$		41.7	21.6	33.3	34.2	3.0
$\text{SiH}_3\text{-SiF} + \text{H}_2 \rightarrow \text{H}_3\text{Si-SiH}_2\text{F}$	36.3	25.8	17.3	17.9	18.9	1.8
$\text{H}_2\text{FSi-SiF} + \text{H}_2 \rightarrow \text{H}_2\text{FSi-SiH}_2\text{F}$	34.2	24.9	16.3	16.9	17.7	2.4
$\text{HSiH} + \text{HF} \rightarrow \text{SiH}_3\text{F}^b$		19.4	-0.1	5.7	3.9	1.0
$\text{H}_3\text{Si-SiH} + \text{HF} \rightarrow \text{H}_3\text{Si-SiH}_2\text{F}$	13.8	18.5	-1.3	5.3	0.1	0.8
$\text{H}_2\text{FSi-SiH} + \text{HF} \rightarrow \text{H}_2\text{FSi-SiH}_2\text{F}$	12.6	19.3	-0.5	6.2	0.9	0.8
$\text{HSiF} + \text{HF} \rightarrow \text{SiH}_2\text{F}_2^b$		22.1	3.5	9.4	7.8	0.3
$\text{H}_3\text{Si-SiF} + \text{HF} \rightarrow \text{HF}_2\text{Si-SiH}_3$	15.9	20.0	1.7	7.9	3.2	0.1
$\text{H}_3\text{Si-H} + \text{SiH}_2 \rightarrow \text{H}_3\text{Si-SiH}_3$	20.7	11.1	-1.9	-1.0	-1.2	2.5
$\text{H}_2\text{FSi-H} + \text{SiH}_2 \rightarrow \text{H}_2\text{FSi-SiH}_2\text{F}$	15.2	5.4	-8.8	-7.4	-8.3	2.3
$\text{HF}_2\text{Si-H} + \text{SiH}_2 \rightarrow \text{HF}_2\text{Si-SiH}_3$	17.7	9.1	-5.1	-3.8	-4.8	2.0
$\text{H}_3\text{Si-H} + \text{SiHF} \rightarrow \text{H}_3\text{Si-SiH}_2\text{F}$	32.4	23.0	12.7	13.2	13.0	1.9
$\text{H}_2\text{FSi-H} + \text{SiHF} \rightarrow \text{H}_2\text{FSi-SiH}_2\text{F}$	30.6	21.0	9.8	10.7	9.8	1.4
$\text{H}_3\text{Si-H} + \text{SiF}_2 \rightarrow \text{HF}_2\text{Si-SiH}_3$	54.2	44.4	38.2	38.2	38.5	1.1
$\text{H}_3\text{Si-F} + \text{SiH}_2 \rightarrow \text{H}_3\text{Si-SiH}_2\text{F}$	10.8	15.8	1.2	4.2	2.1	3.0
$\text{H}_2\text{FSi-F} + \text{SiH}_2 \rightarrow \text{H}_2\text{FSi-SiH}_2\text{F}$	9.7	13.7	-1.4	1.7	-0.4	2.3
$\text{H}_3\text{Si-F} + \text{SiHF} \rightarrow \text{HF}_2\text{Si-SiH}_3$	11.4	17.9	4.5	7.2	5.2	2.2

<sup>a</sup> In kcal/mol with  $\Delta ZPE$  included. <sup>b</sup> From ref 5, MP4 values do not include triples.

TABLE III: Isodesmic Reactions Used To Compute the Heats of Formation of the Fluorodisilanes and Silylsilylenes<sup>a</sup>

reactions	3-21G	6-31G*				3-21G	molecule, $\Delta H_f^\circ$
	HF	HF	MP2	MP3	MP4	$\Delta ZPE$	
$\text{H}_3\text{Si-SiH}_2\text{F} + 2\text{SiH}_4 \rightarrow \text{Si}_2\text{H}_6 + \text{SiH}_3\text{F} + \text{SiH}_4$	-1.5	-1.2	-1.0	-1.2	-0.8	0.4	$\text{H}_3\text{Si-SiH}_2\text{F}$ , -73.4
$\text{H}_3\text{Si-SiHF}_2 + 2\text{SiH}_4 \rightarrow \text{Si}_2\text{H}_6 + \text{SiH}_2\text{F}_2 + \text{SiH}_4$	-2.4	-1.4	-1.1	-1.4	-0.8	0.9	$\text{H}_3\text{Si-SiHF}_2$ , -174.0
$\text{H}_2\text{FSi-SiH}_2\text{F} + 2\text{SiH}_4 \rightarrow \text{Si}_2\text{H}_6 + 2\text{SiH}_3\text{F}$	-4.7	-2.5	-2.5	-2.7	-2.0	0.9	$\text{H}_2\text{FSi-SiH}_2\text{F}$ , -166.2
$\text{H}_3\text{Si-SiH} + \text{SiH}_4 \rightarrow \text{Si}_2\text{H}_6 + \text{SiH}_2$	-0.6	-0.5	0.1	0.0	0.0	-0.7	$\text{H}_3\text{Si-SiH}$ , 74.8
$\text{H}_2\text{FSi-SiH} + \text{SiH}_4 \rightarrow \text{H}_2\text{FSi-SiH}_3 + \text{SiH}_2$	-1.7	-0.1	0.6	0.7	0.6	-0.7	$\text{H}_2\text{FSi-SiH}$ , -19.1
$\text{HF}_2\text{Si-SiH} + \text{SiH}_4 \rightarrow \text{HF}_2\text{Si-SiH}_3 + \text{SiH}_2$	-5.1	-1.8	-1.3	-1.4	-1.4	-0.7	$\text{HF}_2\text{Si-SiH}$ , -117.6
$\text{H}_3\text{Si-SiF} + \text{SiH}_4 \rightarrow \text{Si}_2\text{H}_6 + \text{SiHF}$	-2.9	-3.0	-2.1	-2.4	-1.6	-0.0	$\text{H}_3\text{Si-SiF}$ , -26.4
$\text{H}_2\text{FSi-SiF} + \text{SiH}_4 \rightarrow \text{H}_2\text{FSi-SiH}_3 + \text{SiHF}$	-5.6	-3.3	-2.7	-2.8	-2.2	0.0	$\text{H}_2\text{FSi-SiF}$ , -119.0

<sup>a</sup> In kcal/mol with  $\Delta ZPE$  included.

Barriers for insertion reactions are given in Table II. Table III presents the data for isodesmic reactions used to calculate the heats of formation of the fluorodisilanes and silylsilylenes; Table IV summarizes the thermal decomposition barriers.

**Geometries.** The structures of the disilane reactants and products are shown in Figures 1 and 2; the geometries of the monosilanes have been discussed previously.<sup>5</sup> The effect of fluorine substitution on disilane is relatively minor. The bonds adjacent to the fluorine are slightly shorter; the F-Si-Si and F-Si-H angles are somewhat smaller than their hydrogen analogues. For 1,2-difluorosilane, the gauche and anti conformers are equal in energy ( $E_{\text{gauche}} - E_{\text{trans}} = -0.2$  and  $0.3$  kcal/mol at HF/3-21G and HF/6-31G\*, respectively). In the silylsilylenes, fluorine substitution on the divalent silicon opens the angle by ca.  $4.5^\circ$ , similar to the monosilylenes,  $\text{SiH}_{2-n}\text{F}_n$ . For the 2-fluoro-, 1,2-difluoro- and 2,2-difluorosilylenes, the conformers with the silylene lone pair syn to an Si-F bond are slightly favored.

The geometry of the transition state for silylsilylene insertion into  $\text{H}_2$  (Figure 3a) is essentially the same as that of  $\text{SiH}_2 + \text{H}_2$  in terms of the distances and angles between the silylene and  $\text{H}_2$ . Fluorine substitution on the silyl group has very little effect on the transition-state geometry (other rotomers may also be first-order saddle points). Similarly, the transition structures for the ipso fluorosilylsilylenes (Figure 3d,e) are close analogues of  $\text{SiHF} + \text{H}_2$ . The transition states for fluorosilylsilylene insertion into HF, Figure 4, closely resemble that of  $\text{SiXY} + \text{HF}$ <sup>5</sup> and can also be expected to form a cluster with HF prior to the transition state for insertion.

Figure 5 shows the transition structures for silylene insertion into an SiH bond or, correspondingly, the transition structures for disilane decomposition into a silylene and a monosilane. These structures can also be viewed as a 1,2-hydrogen shift across an

TABLE IV: Thermal Decomposition Barriers of  $\text{Si}_2\text{H}_6-n\text{F}_n$  ( $n = 1, 2$ )<sup>a</sup>

reaction	$\Delta H_f^\circ$	barrier	
		forward	reverse
$\text{H}_3\text{Si-SiH}_3$			
$\rightarrow \text{H}_3\text{Si-SiH} + \text{H}_2$	55	55	-3
$\rightarrow \text{SiH}_4 + \text{SiH}_2$	56	56	-1
$\rightarrow \text{SiH}_3 + \text{SiH}_3$	76	76	0
$\rightarrow \text{H}_2\text{Si=SiH}_2 + \text{H}_2$	47	86	39
$\text{H}_3\text{Si-SiHF}_2$			
$\rightarrow \text{H}_2\text{FSi-SiH} + \text{H}_2$	54	54	-4
$\rightarrow \text{H}_3\text{Si-SiF} + \text{H}_2$	47	56	9
$\rightarrow \text{H}_3\text{Si-SiH} + \text{HF}$	83	86	3
$\rightarrow \text{SiH}_3\text{F} + \text{SiH}_2$	55	55	-8, 2
$\rightarrow \text{SiH}_4 + \text{SiHF}$	47	60	13
$\rightarrow \text{SiH}_3 + \text{SiH}_2\text{F}$	78	78	0
$\text{H}_3\text{Si-SiHF}_2$			
$\rightarrow \text{HF}_2\text{Si-SiH} + \text{H}_2$	56	56	-6
$\rightarrow \text{H}_3\text{Si-SiF} + \text{HF}$	83	89	6
$\rightarrow \text{SiH}_2\text{F}_2 + \text{SiH}_2$	55	55	-5, 0
$\rightarrow \text{SiH}_3\text{F} + \text{SiHF}$	53	58	5
$\rightarrow \text{SiH}_4 + \text{SiF}_2$	32	71	39
$\rightarrow \text{SiH}_3 + \text{SiHF}_2$	81	81	0
$\text{H}_2\text{FSi-SiH}_2\text{F}$			
$\rightarrow \text{H}_2\text{FSi-SiF} + \text{H}_2$	47	54	7
$\rightarrow \text{H}_2\text{FSi-SiH} + \text{HF}$	82	86	4
$\rightarrow \text{SiH}_2\text{F}_2 + \text{SiH}_2$	48	48	0
$\rightarrow \text{SiH}_3\text{F} + \text{SiHF}$	45	50	5, 10
$\rightarrow \text{SiH}_2\text{F} + \text{SiH}_2\text{F}$	79	79	0

<sup>a</sup> In kcal/mol; data for  $\text{Si}_2\text{H}_6 \rightarrow \text{H}_2\text{Si=SiH}_2 + \text{H}_2$  taken from ref 6.

Si-Si bond, followed by dissociation into a silylene and a silane. The Si-Si bond is elongated by 0.1-0.2 Å, and the migrating

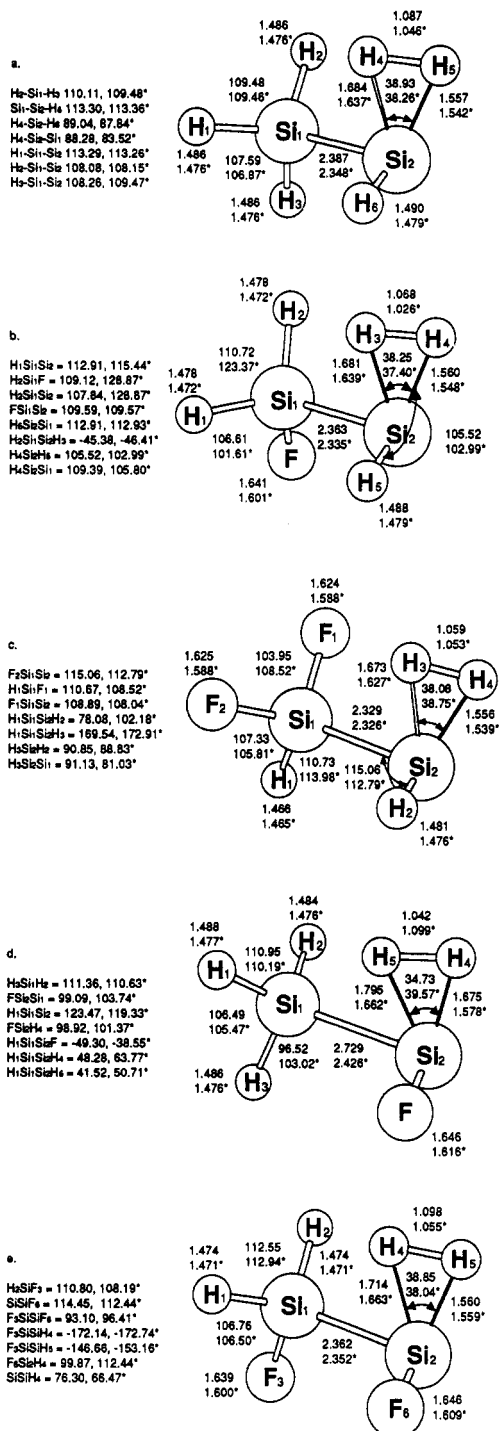


Figure 3. Optimized geometries of the transition states for insertion into  $\text{H}_2$ : no superscript, HF/3-21G; asterisk, HF/6-31G\*.

hydrogen sits approximately above the midpoint of the bond. As shown in Scheme I, four generic conformations (A-E) can be constructed for the parent silylene insertion,  $\text{SiH}_2 + \text{SiH}_4$ . At the Hartree-Fock level, the insertion barrier is lower for the hydrogen migrating to the empty  $p_z$  orbital of the silylene (structures A and C) than for the hydrogen migrating to the filled lone pair (structures D and E); of the two rotomers, the syn orientation between the silyl Si-H bond and the migrating hydrogen (structure A) is lower than the anti (structure C). However, structures A, C, and D are all second-order saddle points (i.e. two imaginary frequencies) at both the HF/3-21G and HF/6-31G\* levels. The lowest energy transition state at the HF level, structure B (also shown in Figure 5a), has  $C_1$  symmetry and can be obtained from structure A by rotating  $10-25^\circ$  about the Si-Si bond. At the MP2 level, the  $\text{SiH}_2 + \text{SiH}_4$  insertion takes place without a barrier<sup>7</sup> or via a transition state with an energy

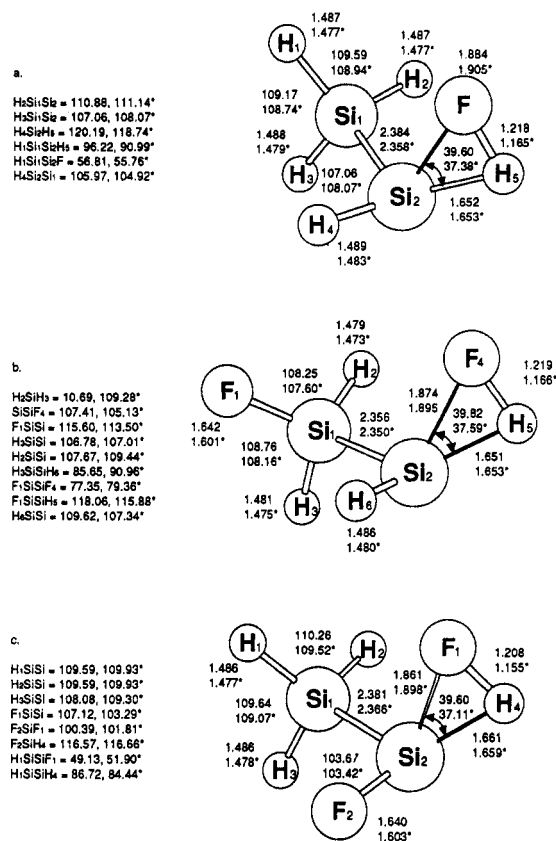
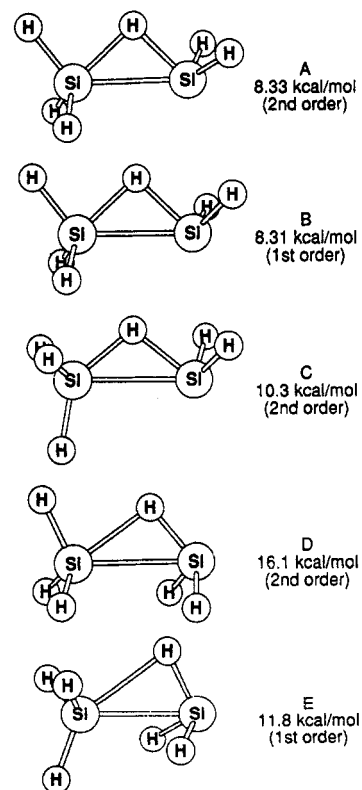
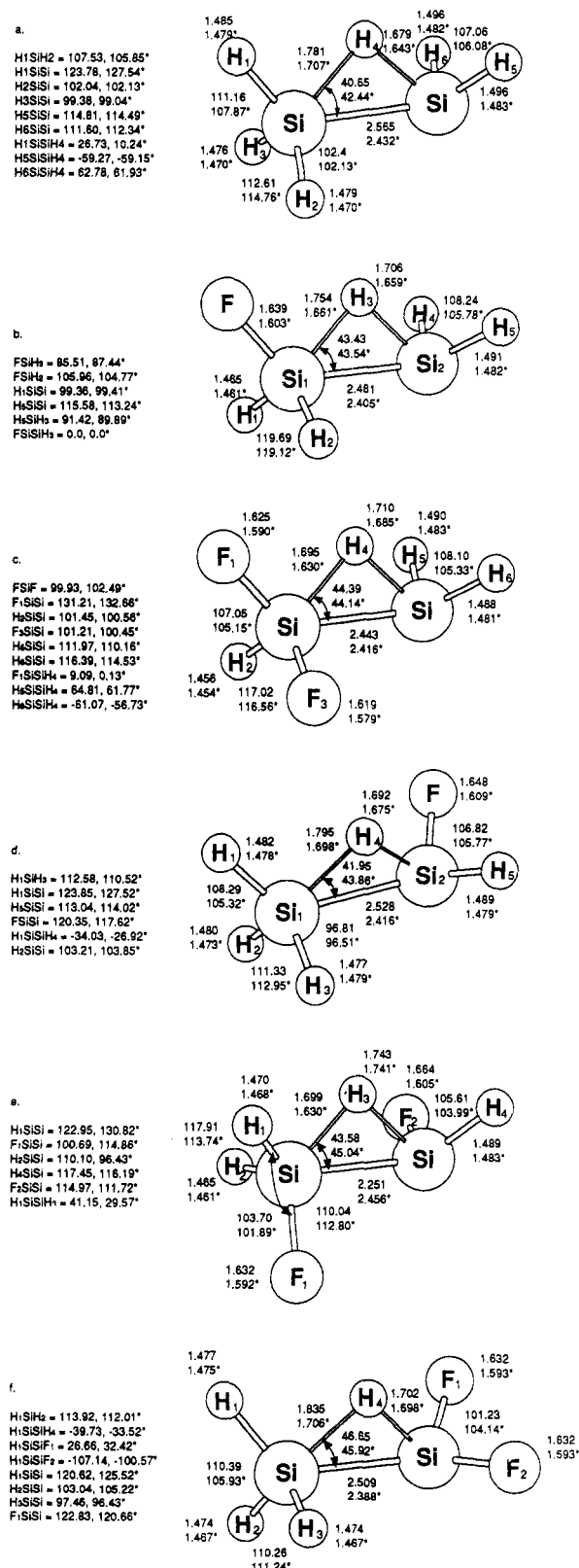


Figure 4. Optimized geometries of the transition states for insertion into HF: no superscript, HF/3-21G; asterisk, HF/6-31G\*.

#### SCHEME I: Conformations and HF/6-31G\* Barriers for $\text{SiH}_2 + \text{SiH}_4$ Insertion



lower than that of the reactants (see Table II). The fluorine-substituted transition states, Figure 5b-f, are derived from structure A of Scheme I and each possesses only one imaginary frequency. Fluorine substitution has surprisingly little effect on the geometry of the transition states. The transition structures with a fluorine syn to the migrating hydrogen are more stable than



**Figure 5.** Optimized geometries of the transition states for insertion into Si-H bonds: no superscript, HF/3-21G; asterisk, HF/6-31G\*.

the other rotomers. For  $\text{H}_2\text{FSi-H} + \text{SiH}_2$ , the syn rotomer is more stable than the gauche by 3.6 and 4.5 kcal/mol at HF/3-21G and HF/6-31G\* levels, respectively; for  $\text{HF}_2\text{Si-H} + \text{SiH}_2$ , the syn, gauche structure is 4.2 and 2.9 kcal/mol more stable than the gauche, gauche at HF/3-21G and HF/6-31G\* levels, respectively.

Figure 6 shows the transition states for silylene insertion into Si-F bonds. The parent reaction  $\text{SiH}_2 + \text{SiH}_3\text{F}$  has been studied previously.<sup>7</sup> Like the insertions into SiH bonds, these reactions

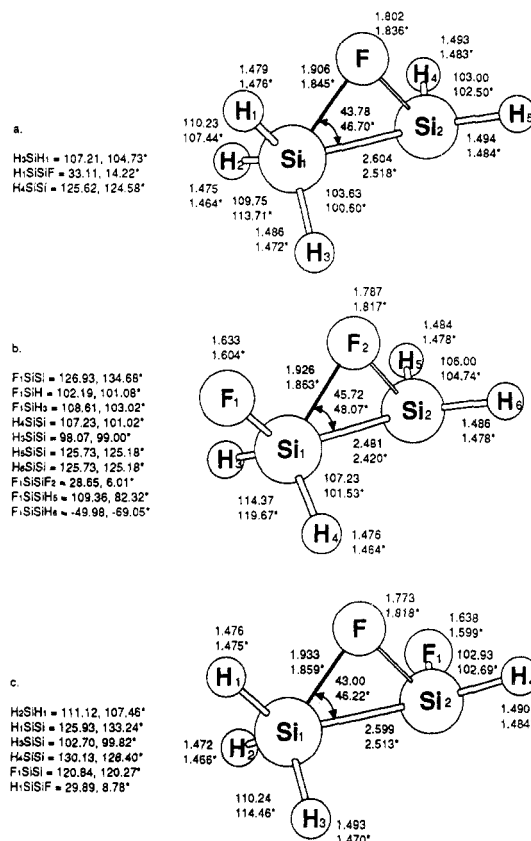
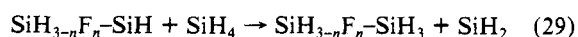
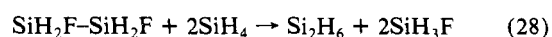
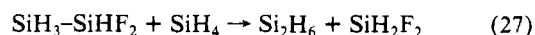
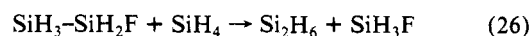


**Figure 6.** Optimized geometries of the transition states for insertion into Si-F bonds: no superscript, HF/3-21G; asterisk, HF/6-31G\*.

can also be described as 1,2-migrations. The fluorine is situated over the middle of the Si-Si bond approximately equidistant from the two silicons. The elongation of the Si-Si bond is similar to those of the transition states for insertion into Si-H. The effect of fluorine substitution on the transition-state geometry is small (other rotamers may also be first-order saddle points).

**Insertion Barriers.** The computed barriers for insertion reactions are collected in Table II. The barrier for insertion into  $\text{H}_2$  is ca. 5 kcal/mol lower with  $\text{SiH}_3\text{SiH}$  than with  $\text{SiH}_2$ ; fluorine substitution of the silyl group lowers the barrier by another 1-2 kcal/mol per fluorine. By contrast, the barrier for  $\text{SiH}_3\text{SiF} + \text{H}_2$  insertion is 20 kcal/mol lower than that of  $\text{SiHF} + \text{H}_2$ , suggesting that the electron-donating ability of the  $\text{SiH}_3$  group counteracts to a large extent the electron-withdrawing/barrier-raising property of the ipso fluoro substitution discussed previously.<sup>5</sup> By contrast, the change in the barrier for insertion into HF is relatively small (2-4 kcal/mol) when  $\text{SiH}_2$  is replaced by  $\text{SiH}_2\text{SiH}$  or  $\text{SiH}_2\text{FSiH}$  and when  $\text{SiHF}$  is replaced by  $\text{SiH}_3\text{SiF}$ . The barriers for  $\text{SiH}_2$  or  $\text{SiHF}$  insertion into either an Si-H bond or an Si-F bond in  $\text{SiH}_4-n\text{F}_n$  appear to decrease with increasing fluorine substitution of the silane. When insertion into either Si-H or Si-F is possible,  $\text{SiH}_2$  prefers the former but  $\text{SiHF}$  prefers the latter at the level of theory used in this study.

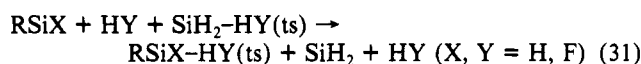
**Heats of Formation.** The experimental and theoretical  $\Delta H_f^\circ$  for the monosilanes were discussed in our earlier paper.<sup>11</sup> The heats of formation of the fluorodisilanes and silylsilylenes in the present study can be determined from the following isodesmic reactions:



The heats of reaction for (26)-(30) are shown in Table III along with the heats of formation derived from these reactions. The

$\Delta H_f^\circ$  for Si<sub>2</sub>H<sub>6</sub> computed at the G2 level of theory<sup>13</sup> ( $\Delta H_f^\circ = 19.8$  kcal/mol) has been used as a reference value. The calculated  $\Delta H_f^\circ$  for SiH<sub>3</sub>SiH (74.8 kcal/mol) is within 2 kcal/mol of the experimental values ( $73 \pm 2$  kcal/mol)<sup>21-23</sup> and the theoretical value computed at the G2 level<sup>13</sup> (73.7 kcal/mol). This suggests that the other heats of formation calculated from reactions 26-30 may have similar error bars.

**Mechanism for Thermal Decomposition.** The data pertinent to the thermal decomposition of the fluorodisilanes is collected in Table IV. The barriers for the reverse reactions were taken from Table II for the silylene insertions or were set to zero for homolytic bond cleavage. Calculations on monosilane decompositions<sup>5</sup> indicate that barriers for silylene insertion into H<sub>2</sub> are too high by 6 kcal/mol at the present level of theory; likewise, insertion barriers involving HF appear to be 4 kcal/mol too low at the present level of theory. The following isodesmic reaction was used to estimate the barriers for H<sub>2</sub> and HF insertions listed in Table IV



based on higher level calculations for SiH<sub>2</sub> + H<sub>2</sub> → SiH<sub>2</sub>-H<sub>2</sub>(ts) (1.7 kcal/mol<sup>24</sup>) and SiH<sub>2</sub> + HF → SiH<sub>2</sub>-HF(ts) (6.6 kcal/mol<sup>5</sup>).

The energy profiles for thermal decomposition of the fluorodisilanes are shown in Figure 7. The preferred pathways for decomposition involve 1,1-elimination of H<sub>2</sub> and the extrusion of SiH<sub>2</sub> or SiHF. Homolytic cleavage of the Si-Si bond is typically 15-30 kcal/mol higher; 1,1-elimination of HF is ca. 30 kcal/mol higher. These trends are also expected to hold for more highly fluorinated disilanes.

For Si<sub>2</sub>H<sub>6</sub>, the barriers for decomposition into SiH<sub>3</sub>SiH + H<sub>2</sub> and SiH<sub>2</sub> + SiH<sub>4</sub> are approximately equal. In Si<sub>2</sub>H<sub>5</sub>F, the barrier heights for SiH<sub>2</sub>FSiH + H<sub>2</sub>, SiH<sub>3</sub>SiF + H<sub>2</sub>, and SiH<sub>2</sub> + SiH<sub>3</sub>F (the reverse of insertion into the SiH bond) are nearly the same. The path leading to SiHF + SiH<sub>4</sub> lies ca. 5 kcal/mol higher. The 1,1-elimination barrier of HF is very high, solely due to the heat of the reaction (83 kcal/mol). Gordon et al.<sup>6</sup> and Curtiss et al.<sup>13</sup> have calculated that SiH<sub>2</sub>=SiH<sub>2</sub> is 7-9 kcal/mol more stable than SiH<sub>3</sub>SiH. Hence the  $\Delta H_r^\circ$  for 1,2-elimination of HF is ca. 74-76 kcal/mol. The barrier for SiH<sub>2</sub>=SiH<sub>2</sub> + H<sub>2</sub> 1,2-addition is ca. 40 kcal/mol; this suggests that the barrier for 1,2-elimination of HF may be 20-40 kcal/mol higher than the heat of reaction (e.g. a barrier of 95-115 kcal/mol). Thus reactions involving 1,2-elimination of H<sub>2</sub> or HF are not considered further.

The barrier heights for decomposition of Si<sub>2</sub>H<sub>4</sub>F<sub>2</sub> depend on whether the fluorine substitution is 1,1 or 1,2. As is evident from the difference in the heats of formation of the two isomers ( $\Delta\Delta H_f^\circ = 7.8$  kcal/mol, Table III) and from bond separation reactions such as SiH<sub>4</sub> + SiH<sub>2</sub>F<sub>2</sub> → 2SiH<sub>3</sub>F ( $\Delta H_r^\circ = 6.4$  kcal/mol<sup>11</sup>), there is a special stabilization when two fluorines are attached to the same center (for a discussion of this effect, see ref 25). For H<sub>3</sub>Si-SiHF<sub>2</sub>, the lowest energy channels lead to HF<sub>2</sub>Si-SiH + H<sub>2</sub> and to SiH<sub>2</sub> + SiH<sub>2</sub>F<sub>2</sub> with SiHF + SiH<sub>3</sub>F a few kcal/mol higher; for H<sub>2</sub>FSi-SiH<sub>2</sub>F decomposition, the SiH<sub>2</sub> + SiH<sub>2</sub>F<sub>2</sub>, H<sub>2</sub>FSi-SiF + H<sub>2</sub>, and SiHF + SiH<sub>3</sub>F pathways are nearly equal.

### Summary

The pathways for thermal decomposition of fluorodisilanes have been examined by ab initio molecular orbital methods. Barriers for homolytic bond cleavage have been obtained from calculated heats of formation of reactants and products. Earlier studies showed that 1,2-elimination reactions have very high barriers; hence they were not considered explicitly. The remaining path-

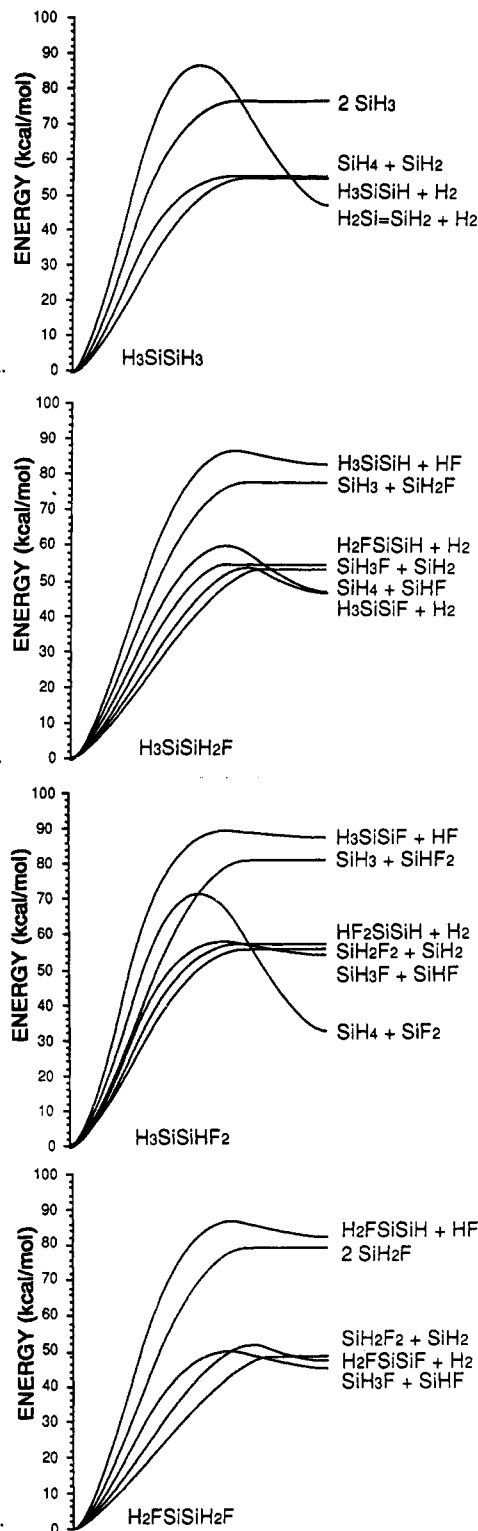


Figure 7. Energy profiles for the unimolecular decomposition of fluorodisilanes (data from Table IV).

ways, 1,1-elimination of H<sub>2</sub> or HF and extrusion of SiXY (X, Y = H, F), are the reverse of silylene insertion reactions. The transition structures for the insertion of SiH<sub>3-n</sub>F<sub>n</sub>SiH and SiH<sub>3-n</sub>F<sub>n</sub>SiF into H<sub>2</sub> and HF closely resemble the transition structures for SiH<sub>2</sub> and SiHF plus H<sub>2</sub> and HF. The transition states for the insertion of SiXY (X, Y = H, F) into Si-H and Si-F bonds have structures that can best be described as 1,2-migration of H or F across the Si-Si bond in the product disilane. Fluorine substitution on the silyl group has a relatively small effect on the structures of the transition states for insertion reactions. Ipso fluorine substitution of silylsilylenes raises the insertion barriers but not as much as for the monosilylenes, apparently because of the electron-donating ability of the silyl group. The preferred

(21) Walsh, R. *Acc. Chem. Res.* **1981**, *14*, 246.

(22) Walsh, R. *The Chemistry of Organic Silicon Compounds*; Patai, S., Rappoport, Z., Eds. Wiley: New York, 1989; Chapter 5.

(23) Martin, G.; O'Neal, H. E.; Ring, M. A. *Int. J. Chem. Kinet.* **1990**, *22*, 613.

(24) Gordon, M. S.; Gano, D. R.; Frisch, M. J.; Binkley, J. S. *J. Am. Chem. Soc.* **1986**, *108*, 2191.

(25) Dill, J. D.; Schleyer, P. v. R.; Pople, J. A. *J. Am. Chem. Soc.* **1976**, *98*, 1663. Ignacio, E. W.; Schlegel, H. B. *J. Phys. Chem.*, submitted for publication.

pathways for thermal decomposition of the fluorodisilanes involve 1,1-elimination of H<sub>2</sub> and extrusion of SiH<sub>2</sub> or SiHF from RSiH<sub>2-n</sub>F<sub>n</sub> groups. Products with multiple fluorines on the same tetravalent center appear to be preferred over products with fluorines on different centers.

**Acknowledgment.** We wish to thank the Wayne State University Computing Services and the Pittsburgh Supercomputer Center for generous allocations of computer time. This work was supported by a grant from the National Science Foundation (Grant CHE 90-20398).

## Transition-State Properties for the Reaction of Hydroxyl Radicals with Methane

Sarah A. L. Jones and Philip D. Pacey\*

Department of Chemistry, Dalhousie University, Halifax, Nova Scotia, Canada B3H 4J3  
(Received: July 17, 1991; In Final Form: October 28, 1991)

Experimental data have been collected from a review of relevant literature regarding the temperature dependence of the rate constant for transfer of a hydrogen atom from methane to hydroxyl. Transition-state theory expressions were fitted to the data by least squares methods to determine three parameters: the mean of four low-frequency vibrational term values in the transition species,  $\omega_b = 570 \pm 20 \text{ cm}^{-1}$ , the characteristic tunneling temperature, which was less than 200 K, and the effective height of the activation barrier,  $V_b = 19 \pm 2 \text{ kJ mol}^{-1}$ .

### Introduction

The reaction



plays a central role in the combustion of natural gas. Consequently, the reaction has been the subject of many experimental kinetic studies,<sup>1-17</sup> over a wide range of temperatures. The Arrhenius plot for the reaction is curved. This presents an opportunity to learn more from the temperature dependence than just the usual two Arrhenius parameters. A modified Arrhenius expression with an extra factor of  $T^n$  has previously been fitted to the data,<sup>7,9,12,18</sup> but the parameters determined did not have simple physical significance. An alternative, which is explored in the

TABLE I: Summary of Input Parameters

$\omega_b$ , $\text{cm}^{-1}$	1306
$I_{\text{CH}_4}$ , $\text{g } \text{Å}^2 \text{ mol}^{-1}$	3.20
$I_{\text{OH}}$ , $\text{g } \text{Å}^2 \text{ mol}^{-1}$	0.89
$\Delta$ , $\text{cm}^{-1}$	139.7
$V_{\text{br}} - V_b$ , $\text{kJ mol}^{-1}$	61.4
$\delta$	4
$(I_X I_Y I_Z)_{\text{TS}}$ , $\text{g}^3 \text{Å}^6 \text{ mol}^{-3}$	$1.34 \times 10^4$
$I_{\text{R}}$ , $\text{g } \text{Å}^2 \text{ mol}^{-1}$	0.67

present article, is to fit a transition-state theory (TST) model<sup>19</sup> to the kinetic data.

The first two parameters obtained from this model are the effective barrier height,  $V_b$ , and the mean, transitional, vibrational term value,  $\omega_b$ . To deal with the change of vibrational frequencies from reactants to transition state to products, it is assumed that several vibrational partition functions do not change significantly and that the remaining transitional vibrations may be combined in an average, low-frequency term value for the transition species. This three-parameter TST model also incorporates the notion of tunneling through the barrier with a characteristic tunneling temperature,  $T^*$ . This parameter,  $T^*$ , can be related to the second derivative of the barrier top by means of the equation

$$T^* = hc\omega^*/2\pi k_B \quad (1)$$

where  $h$  is Planck's constant,  $c$  the speed of light,  $k_B$  Boltzmann's constant, and  $\omega^*$  the term value for vibration in a well created by inverting the barrier.<sup>19</sup>

In order to obtain these three parameters  $V_b$ ,  $T^*$ , and  $\omega_b$  from the TST model, several properties of the reactants and transition state must be known. Moments of inertia and vibrational frequencies of the reactants were obtained from spectroscopic sources.<sup>20</sup> Moments of inertia for the transition state were calculated from a semiempirical bond energy-bond order (BEBO) estimation.<sup>16</sup>

This method has previously been applied to several other reactions.<sup>19,21,22</sup> It has consistently provided transition-state

(1) Wilson, W. E.; Westenber, A. A. *Symp. (Int.) Combust.*, [Proc.] 1967, 11, 1143-1149.

(2) Greiner, N. R. *J. Chem. Phys.* 1970, 53, 1070-1076.

(3) Davis, D. D.; Fisher, S.; Schiff, R. *J. Chem. Phys.* 1974, 61, 2213-2219.

(4) Margitan, J. J.; Kaufman, F.; Anderson, J. G. *Geophys. Res. Lett.* 1974, 1, 80-81.

(5) Gordon, S.; Mulac, W. A. *Int. J. Chem. Kinet., Symp.* 1975, 1, 289-299.

(6) Overend, R.; Paraskevopoulos, G.; Cvetanovic, R. J. *Can. J. Chem.* 1975, 53, 3374-3382.

(7) Zellner, R.; Steinert, W. *Int. J. Chem. Kinet.* 1976, 8, 397-409.

(8) Cox, R. A.; Derwent, R. G.; Holt, P. M. *J. Chem. Soc., Faraday Trans. 1* 1976, 72, 2031-2043.

(9) Tully, F. P.; Ravishankara, A. R. *J. Phys. Chem.* 1980, 84, 3126-3130.

(10) Jeong, K.-M.; Kaufman, F. *J. Phys. Chem.* 1982, 86, 1808-1815.

(11) Baulch, D. L.; Craven, R. J. B.; Din, M.; Drysdale, D. D.; Grant, S.; Richardson, D. J.; Walker, A.; Watling, G. *J. Chem. Soc., Faraday Trans. 1* 1983, 79, 689-698.

(12) Madronich, S.; Felder, W. *Symp. (Int.) Combust.*, [Proc.] 1984, 20, 703-711.

(13) Jonah, C. D.; Mulac, W. A.; Zeglinski, P. *J. Phys. Chem.* 1984, 88, 4100-4104.

(14) Smith, G. P.; Fairchild, P. W.; Jeffries, J. B.; Crosley, D. R. *J. Phys. Chem.* 1985, 89, 1269-1278.

(15) Bott, J. F.; Cohen, N. *Int. J. Chem. Kinet.* 1989, 21, 485-498.

(16) Ernst, J.; Wagner, H.; Zellner, R. *Ber. Bunsen-Ges. Phys. Chem.* 1978, 82, 409-414.

(17) Howard, C. J.; Evenson, K. M. *J. Chem. Phys.* 1976, 64, 197-201.

(18) Zellner, R. *J. Phys. Chem.* 1979, 83, 18-23.

(19) Furue, H.; Pacey, P. D. *J. Phys. Chem.* 1990, 94, 1419-1425.

(20) Chase, M.; Davies, C.; Downey, J.; Frurip, D.; McDonald, A.; Szyverud, A. JANAF Thermochemical Tables. *J. Phys. Chem. Ref. Data, Suppl. 1* 1985, 14, 595, 596, 1248, 1274.